

Retinal Artery and Vein Classification via Dominant Sets Clustering-based Vascular Topology Estimation

Yitian Zhao¹, Jianyang Xie^{1,2}, Pan Su³, Yalin Zheng⁴, Yonghuai Liu⁵, Jun Cheng¹, Jiang Liu¹

¹ Cixi Institute of Biomedical Engineering, Ningbo Institute of Industrial Technology, Chinese Academy of Sciences; ² School of Optics and Electronics, Beijing Institute of Technology; ³ School of Control and Computer Engineering, North China Electric Power University; ⁴ Department of Eye and Vision Science, Liverpool University; ⁵ Department of Computer Science, Aberystwyth University

Abstract. The classification of the retinal vascular tree into arteries and veins is important in understanding the relation between vascular changes and a wide spectrum of diseases. In this paper, we have proposed a novel framework that is capable of making the artery/vein (A/V) distinction in retinal color fundus images. We have successfully adapted the concept of *dominant sets clustering* and formalize the retinal vessel topology estimation and the A/V classification problem as a pairwise clustering problem. Dominant sets clustering is a graph-theoretic approach that has been proven to work well in data clustering. The proposed approach has been applied to three public databases (INSPIRE, DRIVE and VICAVR) and achieved high accuracies of 91.0%, 91.2%, and 91.0%, respectively. Furthermore, we have made manual annotations of vessel topologies from these databases, and this annotation will be released for public access to facilitate other researchers in the community to do research in the same and related topics.

Keywords: Artery/vein classification, dominant sets, vessel, topology

1 Introduction

Automated analysis of retinal vascular structure is very important to support examination, diagnosis and treatment of eye disease [1, 2]. Vascular changes in the eye fundus images, such as the arteriolar constriction or arteriovenous nicking, are also associated with diabetes, cardiovascular diseases and hypertension [3]. Arteriolar-to-Venular Ratio (AVR) is considered to be an important characteristic sign of a wide spectrum of diseases [4]. Low AVR, i.e., narrowing in arteries and widening of veins, is a direct biomarker for diabetic retinopathy. By contrast, a high AVR has been associated with higher cholesterol levels and inflammatory markers [5]. However, manual annotation of the artery and vein vessels is time consuming and prone to human errors. An automated method for classification of vessels as arteries or veins is indispensable.

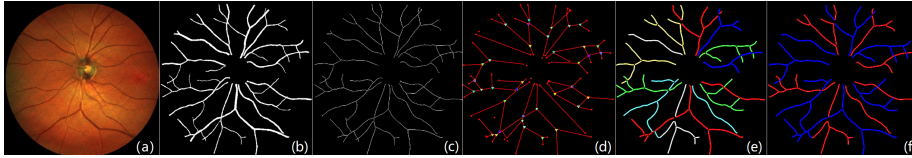


Fig. 1: Overview of the proposed method. (a) Original image. (b) Extracted vessels. (c) Skeletonized vessels. (d) Graph generated with significant nodes overlaid. (e) Estimated vascular network topology. (f) Classified arteries and veins, where arteries are shown in red and veins in blue.

The task of separating vascular network into arteries and veins appear to be understudied. Martinez-Perez et al. [6] proposed a semi-automatic retinal vessel analysis method that is capable of measuring and quantifying the geometrical and topological properties of retinal vessels. Vazquez et al. [3] combined color-based clustering and vessel tracking to differentiate arteries and veins. A tracking strategy based on the minimal path approach is employed to support the resulting classification by voting. Dashtbozorg et al. [7] proposed a graph-based method for A/V classification. Graph nodes and intensity feature analysis were undertaken to establish the artery/vein distinction. Estrada et al. [5] utilized a global likelihood model to capture the structural plausibility of each vessel, and employed a graph-theoretic method of estimating the overall vessel topology with domain-specific knowledge to accurately classify the A/V types. Huang et al. [8] introduced four new features to avoid distortions resulted from lightness inhomogeneity, and the accuracy of the A/V classification is improved by using a linear discriminate analysis classifier.

Numerous factors can cause the aforementioned A/V classification methods to return inaccurate results. Several methods [3, 6, 8, 9] rely on precise segmentation results: any ambiguity in distinguishing between small and midsized vessels makes the subsequent A/V classification a very difficult computational task. On the other hand, pathological conditions and intensity inhomogenities also affect the performance of A/V classification techniques [7, 8]. To address these problems, we propose a novel Dominant Sets-based A/V classification method (DoS) based on vessel topological features. The underlying vessel topology reveals how the different vessels are anatomically connected to each other, and is able to identify and differentiate the structure of individual vessels from the entire vessel network. The concept of dominant sets clustering [10, 11] was introduced to tackle the problem of vessel topology estimation and A/V classification.

2 Method

Fig. 1 shows a graphical overview of the proposed method.

2.1 Graph Generation

Our proposed topology estimation approach can be applied either on manual annotations or automated segmentation results. The method proposed in [1] was

employed to automatically segment the retinal vessel. An iterative morphology thinning operation [12] is performed on the extracted vessels to obtain a single-pixel-wide skeleton map. The vascular bifurcations/crossovers, and vessel ends (terminal points) can be extracted from the skeleton map by locating intersection points (pixels with more than two neighbors) and terminal points (pixels with one neighbor). All the intersection points and their neighbors may then be removed from the skeleton map, in order to obtain an image with clearly separated vessel segments. A vessel graph can be generated by linking first and last nodes in the same vessel segment. The generated graph usually includes misrepresentations of the vessels: typical errors are *node splitting*, *missing link* and *false link*. Correction of these errors can be achieved by using the strategy proposed in [7]. Red dots in Fig. 1(d) indicate terminal points, green triangle bifurcations, and blue squares intersection or crossover points.

2.2 Dominant Sets Clustering-based Topology Estimation

The topology reconstruction can be achieved by breaking down the graph nodes into four categories (node degrees 2-5): connecting points (2), bifurcation points (3, 4), and crossing/meeting points (3, 4, 5). The number in the bracket indicates the possible number of links connected to each node (node degree). The method proposed by Dashtbozorg et al. [7] is used to handle cases of nodes of degrees 2-3. For nodes of degrees 4 and 5, a classification method based on dominant sets clustering is proposed. The nodes to be classified are represented as an undirected edge-weighted graph with $G = (V, E, \omega)$.

Since we are only taking into account of the pixels around the connecting point, we have $|V| \leq 5$. The edge set $E \subseteq V \times V$ indicates all the possible connections. $\omega : E \rightarrow R_+^*$ is the positive weight function. The symmetric matrix $A = (a_{ij})$ is used to represent the graph G with a weighted adjacency matrix. This non-negative adjacency matrix is defined as:

$$a_{ij} = \begin{cases} \omega(i, j), & \text{if } (i, j) \in E \wedge i \neq j \\ 0 & , \text{ otherwise.} \end{cases} \quad (1)$$

The concept of dominant set is similar to that of maximum clique. In an undirected edge-weighted graph, the weights of edges within a dominant set should be large, representing high internal homogeneity or similarity, while the weights of those linking to the dominant set from outside it will be small [13]. Let $S \subseteq V$ be a nonempty subset of nodes, $i \in S$, and $j \notin S$. Intuitively, the similarity between nodes j and i can be defined as:

$$\phi_S(i, j) = a_{ij} - \frac{1}{|S|} \sum_{k \in S} a_{ik} \quad (2)$$

It is worth noticing that $\phi_S(i, j)$ can be either positive or negative. $\frac{1}{|S|} \sum_{j \in S} a_{ij}$ is the average weighted degree of i with regard to S . It can be observed that $\frac{1}{|S|} \sum_{j \in S} a_{ij} = 0$ for any $S : |S| = 1 \wedge S \subseteq V$, hence $\phi_{\{i\}}(i, j) = a_{ij}$. For each node $i \in S$, the weight of i with regard to S is assigned as:

$$\omega_s(i) = \begin{cases} 1 & \text{if } |S| = 1 \\ \sum_{j \in S \setminus \{i\}} \phi_{S \setminus \{i\}}(j, i) \omega_{S \setminus \{i\}}(j) & \text{otherwise.} \end{cases} \quad (3)$$

where $S \setminus \{i\}$ indicates the node set S excluding the node i . $\omega_S(i)$ demonstrates the overall similarity between node i and the nodes of $S \setminus \{i\}$.

A subset of nodes $S, S \in V$ is called a *dominant set* if the set S satisfies the following two conditions: a) $\omega_S(i) > 0$, for all $i \in S$; and b) $\omega_{S \cup \{i\}}(i) < 0$, for all $i \notin S$ [11]. It is evident from the above properties that a) a dominant set is defined by high internal homogeneity, whereas b) defines the degree of external incoherence. One can find a dominant set by first localizing a solution of the program:

$$\begin{aligned} & \text{maximize } f(\mathbf{x}) = \mathbf{x}'A\mathbf{x} \\ & \text{subject to } \mathbf{x} \in \Delta \end{aligned} \quad (4)$$

where \mathbf{x}' denotes the transposition of \mathbf{x} , $\Delta \subset \mathbb{R}^{|V|}$, and

$$\Delta = \left\{ \sum_{k=1}^{|V|} x_k = 1, \text{ and } x_k \geq 0 \text{ for all } k = 1 \cdots |V| \right\}$$

A strict local solution to the standard quadratic program \mathbf{x} indicates a dominant set S of G , where $x_k > 0$ means that the according node $i_k \in S$. As suggested in [10,11], an effective optimization approach for solving Eqn. (4) is given by the so-called *replicator dynamics*:

$$x_k^{(t+1)} = x_k^{(t)} \frac{(A\mathbf{x}^{(t)})_i}{\mathbf{x}^{(t)'}A\mathbf{x}^{(t)}}, \quad (5)$$

where $k = 1, 2, \dots, |V|$. It has been proven that for any initialization of $\mathbf{x} \in \Delta$, its trajectory will remain in Δ with the increase of iteration t . Since A is symmetric, the objective function $f(x)$ in Eqn. (4) is either strictly increasing, or constant. In practice, the stop criteria of Eqn. (5) can be set either as a maximal number of iteration t of iterations or a minimal increment of $f(x)$ over two consecutive iterations.

In the reconstruction of a vascular network topology, the dominant set is a good method of identifying branches of the vascular tree with nodes whose degree is above 3. In general, the weights of edges within a vessel segment should be large, representing high internal homogeneity, or similarity. By contrast, the weights of edges will be small for two or more different vessel segments, because those on the edges connecting the vessel ends represent high inhomogeneities [10]. Intuitively, the identification of vessel branches is more likely to be carried out by finding the most “dominant” vessel branch first and then finding the second most “dominant” vessel branch (and so on). Therefore, dominant set clustering is adopted in this step to determine the most “dominant” vessel branch pixels around each connecting point and assign them to one vessel segment. The remaining pixels are then assigned to the other vessel segment. Practically, for each vessel segment, a feature vector of 23 features is derived for each vessel segment to generate the symmetric matrix A , and these features are listed in Table 1.

2.3 Artery/vein Classification

After estimating the vessel topology, the complete vessel network is separated into several *subgraphs* with individual labels. The final goal is to assign these

Table 1: List of feature vectors for classification.

No.	Features
1-6	Mean and stand deviation of the intensities within the segment in RGB channels
7-8	Mean and stand deviation of the orientations of each centerline pixels
9-10	Mean and stand deviation of the curvatures of each centerline pixels
11-12	Mean and stand deviation of the vessel diameters of each vessel segment
13-18	Mean and stand deviation of the intensities of centerline pixel under a Gaussian blurring ($\sigma = 4$) in RGB channels
19-23	Entropy of intensity in RGB channels, orientation and curvature of each centerline pixels

labels to one of two classes: artery and vein. Again, the features listed in Table 1 and the DoS classifier are utilized to classify these individual labels into two clusters, A and B . For each subgraph v , the probability of its being A is computed by the number of vessel pixels classified by DoS as A : $P_A^v = n_A^v / (n_A^v + n_B^v)$, where n_A^v is the number of pixels classified as A , and n_B^v is the number of pixels classified as B . For each subgraph, the higher probability is used to define whether the subgraph is assignable to category A or B . Cluster A and B are then assigned as artery and vein, respectively, based on their average intensity in the green channel: a higher average intensity is classified as artery and lower as vein.

3 Experimental Results

The proposed topology estimation and A/V classification method was evaluated on three publicly available datasets: INSPIRE [14], AV-DRIVE [15], and VICAVR [16]. All of these datasets have manual annotations on A/V classification, but no manual annotations of vessel topology were made on these datasets. Therefore, an expert was asked to manually label the topological information of the vascular structure on all the images from these datasets. Each vessel tree is marked with a distinct color, as shown in the second column of Fig. 2.

3.1 Topology Estimation

The two right-hand columns of Fig. 2 illustrate the results of our vascular topology estimation method. Compared with the manual annotations shown in the second column of Fig. 2, it is clear from visual inspection that our method is able to trace most vascular structures correctly: only a few crossing points were incorrectly traced, as shown in the last column of Fig. 2 - the pink squares indicate the incorrectly traced significant points.

To facilitate better observation of the performance of the proposed method, the percentage of the relevant significant points (connecting, bifurcation, and crossing points) that were correctly identified (average accuracy): was calculated as 91.5%, 92.8%, and 88.9% in INSPIRE, AV-DRIVE, and VICAVR, respectively.

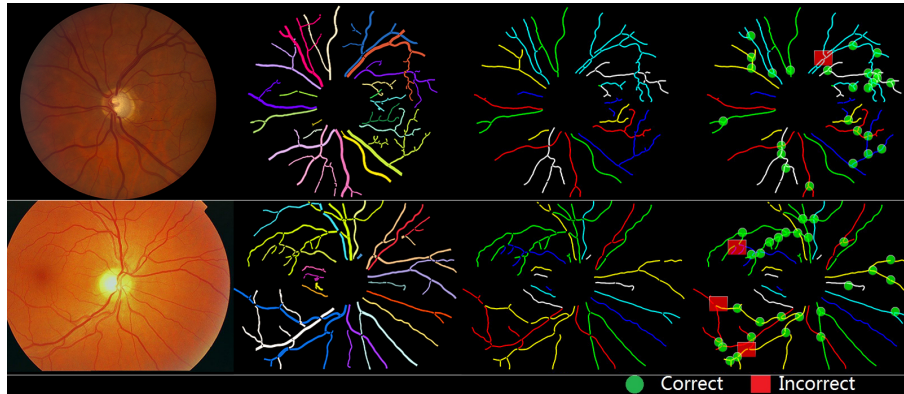


Fig. 2: Examples of vascular topology estimation performances. From left to right column: original image; manual annotations; results from the proposed topology estimation, and the highlighted correct and incorrect connections.

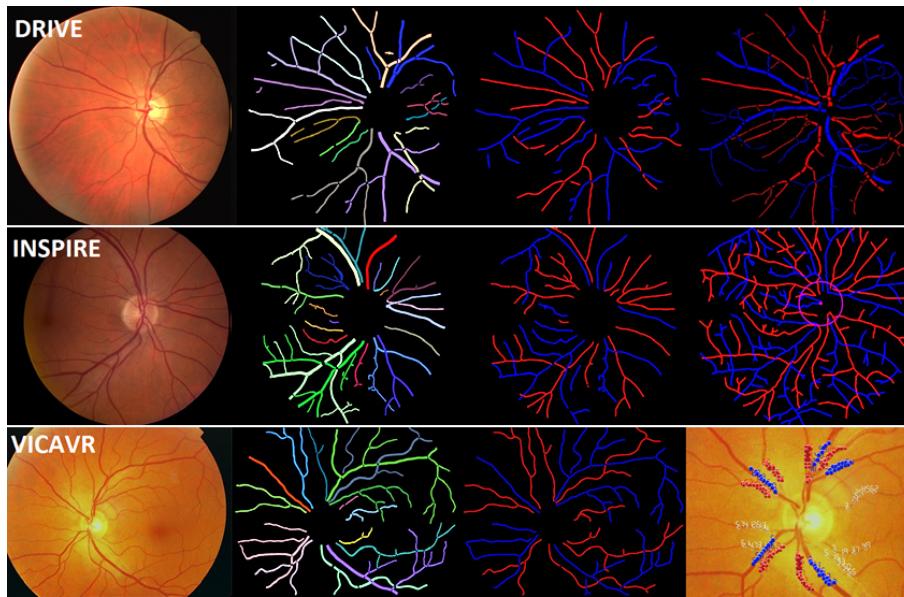


Fig. 3: A/V classification results on three different datasets. From left to right column: original image; vessel topology; A/V classification results of the proposed method; and corresponding manual annotations.

3.2 A/V Classification

Fig. 3 shows the A/V classification performances of the DoS classifier on sample images based on their topological information. Overall, our proposed method correctly distinguished most of the A/V labels on all three datasets, when com-

Table 2: Performances of different A/V classification methods on three datasets.

	INSPIRE			DRIVE [†]		VICAVR [‡]
	Se	Sp	Acc	Se	Sp	Acc
Niemeijer et al. [4]	78.0%	78.0%	-	80.0%	80.0%	-
Vazquez et al. [3]	-	-	-	-	-	88.8%
Dashbozorg et al. [7]	91.0%	86.0%	84.9%	90.0%	84.0%	89.8%
Estrada et al. [5]	91.5%	90.2%	90.9%	91.7%	91.7%	-
Huang et al. [8]	-	-	85.1%	-	-	90.6%
DoS	91.8%	90.2%	91.0%	91.9%	91.5%	91.0%

[†] The compared methods only reported their performances on **Se** and **Sp** on DRIVE.

[‡] The compared methods only reported their performances on **Acc** on VICAVR.

Table 3: Classification results by different classifiers on INSPIRE dataset.

	LDA	QDA	kNN	SVM	DoS
Se	89.6%	90.6%	87.3%	89.9%	91.8%
Sp	84.6%	88.4%	82.6%	88.2%	90.2%
Acc	85.1%	89.2%	83.5%	88.6%	91.0%

pared with the corresponding manual annotations. In order to better demonstrate the superiority of the proposed method, Table 2 reports the comparison of our method with the state-of-the-art methods over three datasets in terms of pixel-wise sensitivity (Se), specificity (Sp), and accuracy (Acc). It is clear that our method outperforms all the compared methods on all datasets, except that the sp score on DRIVE dataset is 0.2% lower than [5].

To highlight the relative performance of our DoS classifier, we also employed commonly-used classifiers, namely linear discriminant analysis (LDA), quadratic discriminant analysis (QDA), support vector machine (SVM) and k-nearest neighbor (kNN) for A/V classification based on the topology-assigned structures derived from images from the INSPIRE dataset, with the same feature vectors as listed in Table 1. It can be seen from Table 3 that our method clearly outperforms the compared classification methods

4 Conclusions

Development of the proposed framework was motivated by medical demands for a tool to measure vascular changes from the retinal vessel network. In this paper, we have proposed a novel artery/vein classification method based on vascular topological characteristics. We utilized the underlying vessel topology to better distinguish arteries from veins. The concept of dominant set clustering was adapted and formalized for topology estimation and A/V classification, as a pairwise clustering problem. The proposed method accurately classified the vessel types on three publicly accessible retinal datasets, outperforming several existing methods. The significance of our method is that it is capable of classifying the whole vascular network, and does not restrict itself to specific regions of

interest. Future work will focus on the AVR calculation based on the proposed methodology.

5 Acknowledgment

This work was supported National Natural Science Foundation of China (61601029, 61602322), Grant of Ningbo 3315 Innovation Team, and China Association for Science and Technology (2016QNRC001).

References

1. Y. Zhao, L. Rada, K. Chen, , and Y. Zheng. Automated vessel segmentation using infinite perimeter active contour model with hybrid region information with application to retinal images. *IEEE Trans. Med. Imaging*, 34(9):1797–1807, 2015.
2. Y. Zhao, Y. Zheng, Y. Liu, Y. Zhao, L. Luo, S. Yang, T. Na, Y. Wang, and J. Liu. Automatic 2-d/3-d vessel enhancement in multiple modality images using a weighted symmetry filter. *IEEE Trans. Med. Imaging*, 37(2):438–450, 2018.
3. S. G. Vázquez, B. Cancela, N. Barreira, G. Coll de Tuero, M. Antònia Barceló, and M. Saez. Improving retinal artery and vein classification by means of a minimal path approach. *Mach. Vis. Appl.*, 24(5):919–930, 2013.
4. M. Niemeijer, X. Xu, A. Dumitrescu, B. van Ginneken, J. Folk, and M. Abramoff. Automated measurement of the arteriolar-to-venular width ratio in digital color fundus photographs. *IEEE Trans. Med. Imaging*, 30(11):1941–1950, 2011.
5. R. Estrada, C. Tomasi, S. Schmidler, and S. Farsiu. Tree topology estimation. *IEEE Trans. Pattern Anal. Mach. Intell.*, 37(8):1688–1701, 2015.
6. M. Martínez-Pérez, A. Hughes, A. Stanton, S. Thom, N. Chapman, A. Bharath, and K. Parker. Retinal vascular tree morphology: a semi-automatic quantification. *IEEE Trans. Biomed. Engineering*, 49(8):912–917, 2002.
7. B. Dashtbozorg, A. M. Mendonça, and A. Campilho. An automatic graph-based approach for artery/vein classification in retinal images. *IEEE Trans. Image Processing*, 23(3):1073–1083, 2014.
8. F. Huang, B. Dashtbozorg, and B. Haar Romeny. Artery/vein classification using reflection features in retina fundus images. *Mach. Vis. Appl.*, 29(1):23–34, 2018.
9. K. Rothaus, X. Jiang, and P. Rhiem. Separation of the retinal vascular graph in arteries and veins based upon structural knowledge. *Image Vision Comput.*, 27(7):864–875, June 2009.
10. M. Pavan and M. Pelillo. Dominant sets and hierarchical clustering. In *9th IEEE Int. Conf. on Computer Vision, 2003*, pages 362–369, 2003.
11. M. Pavan and M. Pelillo. Dominant sets and pairwise clustering. *IEEE Trans. Pattern Anal. Mach. Intell.*, 29(1):167–172, 2007.
12. P. Bankhead, J. McGeown, and T. Curtis. Fast retinal vessel detection and measurement using wavelets and edge location refinement. *PLoS ONE*, 7:e32435, 2009.
13. E. Zemene and M. Pelillo. Interactive image segmentation using constrained dominant sets. In *Europ. Conference on Computer Vision*, pages 278–294, 2016.
14. INSPIRE. <http://webeye.ophth.uiowa.edu/component/k2/item/270>.
15. T. Qureshi, M. Habib, A. Hunter, and B. Al-Diri. A manually-labeled, artery/vein classified benchmark for the drive dataset. In *Proc. IEEE 26th Int. Symp. Computer-Based Med. Syst*, pages 485–488, 2013.
16. VICAVR. <http://www.varpa.es/vicavr.html>.